

LCD-Note-2013-012

Combined Fits of CLIC Higgs Results for the Snowmass Process

Frank Simon*, Marco Szalay*, Philipp Roloff†

* *Max-Planck-Institut für Physik, Munich, Germany,*
† *CERN, Geneva, Switzerland*

September 27, 2013

Abstract

This note presents three combined fits of CLIC Higgs physics results, a model-independent fit based on minimal assumptions and two model-dependent fits assuming that the total width is described by the sum of nine (seven) different visible final states with coupling parameters given by the deviation of the respective partial widths from their SM values. The input values are a snapshot of the CLIC Higgs analyses as of September 2013. The results demonstrate the capabilities of the full three-stage CLIC physics program for a precise exploration of the Higgs sector.

1. Introduction

The CLIC physics program includes a thorough study of the Higgs sector with measurements at all three energy stages, 350 GeV, 1.4 TeV and 3 TeV. These measurements include the model-independent measurement of Higgs production in ZH events, the measurement of decays into fermions and bosons as well as the coupling to the top quark and the self-coupling. To study the impact of this program, the expected precision for all relevant couplings is studied via combined fits, both in a model-independent way and in a model-dependent fit following the strategies used also at the LHC. Since the self-coupling of the Higgs is obtained in a separate analysis and does not contribute to the other couplings it is not considered in the fits presented here. At present, only statistical uncertainties are considered, and theory uncertainties in the model-dependent fit are ignored. Possible correlations of statistical uncertainties (particularly relevant for b, c and g final states) are also not taken into account.

The study is performed in the context of the US Snowmass process to provide input to the Snowmass Higgs working group. The analysis results used as input for the fits are partially preliminary, and reflect the status of the CLIC Higgs analyses as of September 2013.

2. General Fit Strategy

The extraction of the coupling uncertainties is based on χ^2 fits using MINUIT. The model-independent fit has been cross-checked with an independent implementation of a maximum likelihood fit in the Bayesian Analysis Toolkit (BAT) framework, which obtains fully consistent results. Here, only the χ^2 fit is discussed in detail. To perform the fit, a global χ^2 is constructed from the sum of individual χ^2 values for each independent measurement and its respective statistical uncertainty at CLIC. These measurements are either a total cross section σ in the case of the measurement of $e^+e^- \rightarrow \text{ZH}$ via the recoil mass technique or cross section \times branching ratio $\sigma \times BR$ for specific Higgs production modes and decays. To obtain the expected sensitivity for CLIC it is assumed that for all measurements the value expected in the SM has been measured, so only the statistical uncertainties of each measurement are actually used in the χ^2 calculation. The χ^2 for one individual measurement is then given by

$$\chi_i^2 = \frac{(C_i - 1)^2}{\Delta F_i^2}, \quad (1)$$

where C_i is the combination of Higgs couplings (and total width, if applicable) describing the particular measurement, and ΔF_i is the statistical uncertainty of the measurement of the considered process. The full χ^2 then is given by

$$\chi^2 = \sum_i \frac{(C_i - 1)^2}{\Delta F_i^2}. \quad (2)$$

The C_i 's depend on the particular measurements and on the type of fit (model-independent or model-dependent), given in detail below. The results of the individual measurements used in the fits are summarized in Appendix A.

3. Model-independent Fit

The model-independent fit makes minimal assumptions, such as the zero-width approximation to provide the description of the individual measurements in terms of Higgs couplings and of the total width. Here, the C_i 's take the following form: For the total cross section of $e^+e^- \rightarrow \text{ZH}$, it is given by

$$C_{\text{ZH}} = g_{\text{HZZ}}^2, \quad (3)$$

while for specific final states such as $e^+e^- \rightarrow \text{ZH}$, $\text{H} \rightarrow b\bar{b}$ and $e^+e^- \rightarrow \text{H}\nu_e\bar{\nu}_e$, $\text{H} \rightarrow b\bar{b}$ it is given by

$$C_{\text{ZH,H} \rightarrow b\bar{b}} = \frac{g_{\text{HZZ}}^2 g_{\text{H}bb}^2}{\Gamma_{\text{H}}} \quad (4)$$

and

$$C_{H\nu_e\bar{\nu}_e,H\rightarrow b\bar{b}} = \frac{g_{HWW}^2 g_{Hbb}^2}{\Gamma_H}, \quad (5)$$

respectively. The fit is performed with eight free parameters: g_{HZZ} , g_{HWW} , g_{Hbb} , g_{Hcc} , $g_{H\tau\tau}$, $g_{H\mu\mu}$, g_{Htt} and Γ_H .

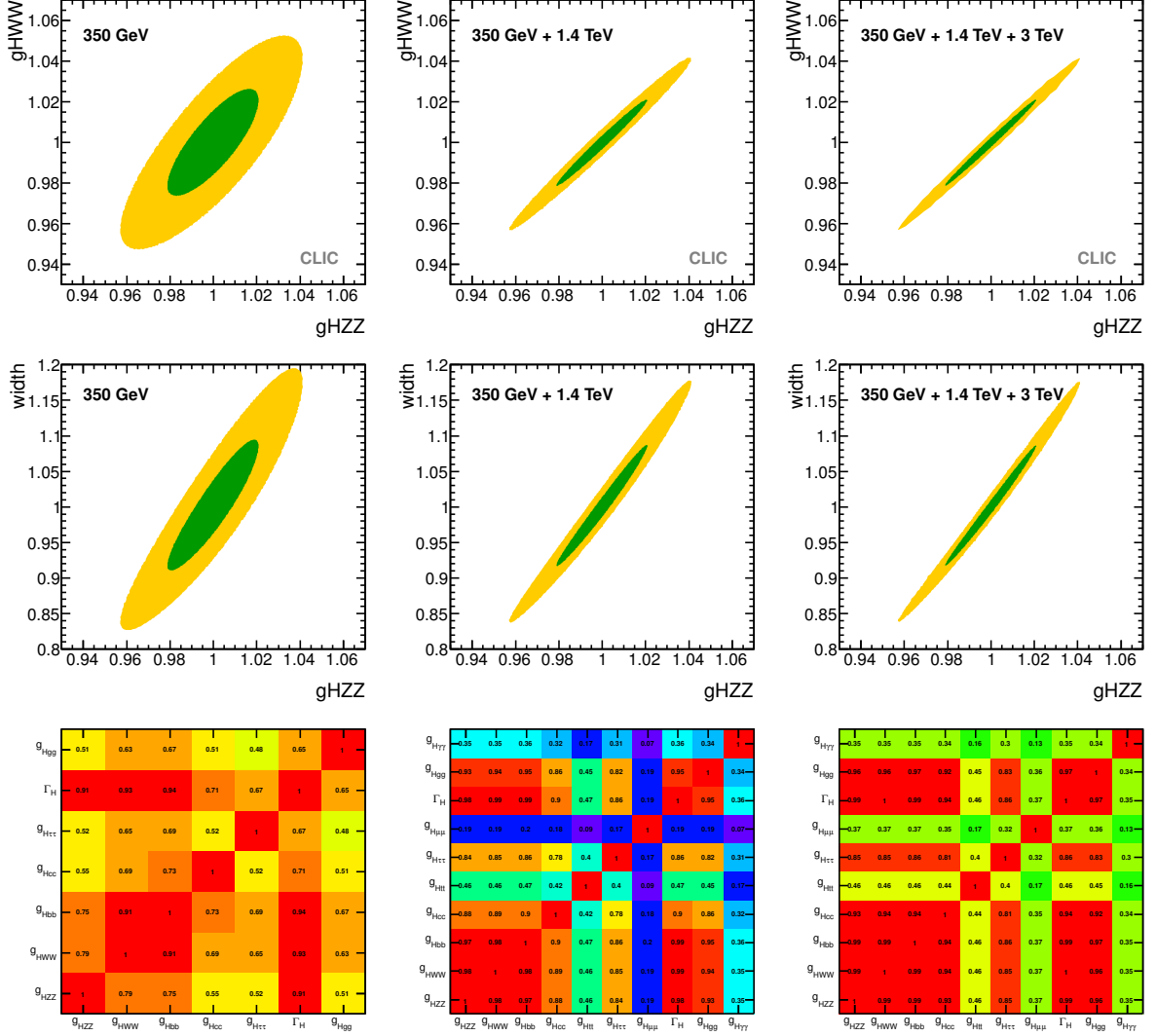


Fig. 1: One and two σ uncertainty contours for g_{HWW} vs g_{HZZ} (top) and total width vs g_{HZZ} (middle). The bottom shows the full correlation matrix of the fit parameters.

The fit is performed in three stages, taking the statistical errors of CLIC at the three considered energy stages (350 GeV, 1.4 TeV, 3 TeV) successively into account. Each new stage also includes all measurements of the previous stages. Figure 1 illustrates the evolution of g_{HZZ} , g_{HWW} and the total width as well as the full correlation matrix of all parameters as more measurements at higher energy become available. A very high degree of correlation of all parameters, in particular those who enter in several measurements with small uncertainties is clearly apparent. Table 1 summarizes the results of the fit. In this fit, the precision of all couplings is ultimately limited by the precision of g_{HZZ} , which is obtained model-independently from the recoil mass measurement.

Table 1: Results of the model-independent fit. Values marked ”-” can not be measured with sufficient precision at the given energy, while values marked ”< ” have not yet been studied at the given energy, but should result in a considerable improvement of the precision. In the case of g_{Htt} , the 3 TeV case has not yet been studied, but is not expected to result in substantial improvement due to the significantly reduced cross-section at high energy.

parameter	precision		
	350 GeV	350 GeV + 1.4 TeV	350 GeV + 1.4 GeV + 3 TeV
g_{HZZ}	2.1%	2.1%	2.1%
g_{HWW}	2.6%	2.1%	2.1%
g_{Hbb}	2.8%	2.2%	2.1%
g_{Hcc}	3.8%	2.4%	2.2%
$g_{H\tau\tau}$	4.0%	2.5%	<2.5%
$g_{H\mu\mu}$	-	11%	5.6%
g_{Htt}	-	4.5%	~4.5%
g_{Hgg}	4.1%	2.3%	2.2%
$g_{H\gamma\gamma}$	-	5.9%	<5.9%
Γ_H	9.2%	8.5%	8.4%

4. Model-dependent fit

For the model-dependent fit, it is assumed that the Higgs decay properties can be described by nine independent parameters κ_{HZZ} , κ_{HWW} , κ_{Hbb} , κ_{Hcc} , $\kappa_{H\tau\tau}$, $\kappa_{H\mu\mu}$, κ_{Htt} , κ_{Hgg} and $\kappa_{H\gamma\gamma}$. These factors are defined by the ratio of the Higgs partial width divided by the partial width expected in the Standard Model as

$$\kappa_i^2 = \frac{\Gamma_i}{\Gamma_i|_{SM}}. \quad (6)$$

In this scenario, the total width is given by the sum of the nine partial widths considered, which is equivalent to assuming no invisible Higgs decays. The variation of the total width from its SM value is thus given by

$$\Gamma_{H,md} = \sum_i \kappa_i^2 BR_i, \quad (7)$$

where BR_i is the SM branching fraction for the respective final state and the subscript “md” stands for “model-dependent”. To obtain these branching fractions, a fixed value for the Higgs mass has to be made. For the purpose of this study, 126 GeV is assumed. The branching ratios are taken from the LHC Higgs cross-section working group, ignoring theoretical uncertainties. To exclude effects from numerical rounding errors, the total sum of BR ’s is normalized to unity.

With these definitions, the C_i ’s in the χ^2 take the following form, analogous to the model-independent fit: For the total cross section of $e^+e^- \rightarrow ZH$, it is given by

$$C_{ZH} = \kappa_{HZZ}^2, \quad (8)$$

while for specific final states such as $e^+e^- \rightarrow ZH, H \rightarrow b\bar{b}$ and $e^+e^- \rightarrow H\nu_e\bar{\nu}_e, H \rightarrow b\bar{b}$ it is given by

$$C_{ZH,H \rightarrow b\bar{b}} = \frac{\kappa_{HZZ}^2 \kappa_{Hbb}^2}{\Gamma_{H,md}} \quad (9)$$

and

$$C_{H\nu_e\bar{\nu}_e,H \rightarrow b\bar{b}} = \frac{\kappa_{HWW}^2 \kappa_{Hbb}^2}{\Gamma_{H,md}}, \quad (10)$$

respectively.

Since at the first energy stage of CLIC no significant measurements of the $H \rightarrow \mu^+ \mu^-$ and $H \rightarrow \gamma\gamma$ decays are possible, the fit is reduced to six free parameters (the coupling to top is also not constrained, but this is without effect on the total width) with an appropriate rescaling of the branching ratios used in the total width for 350 GeV.

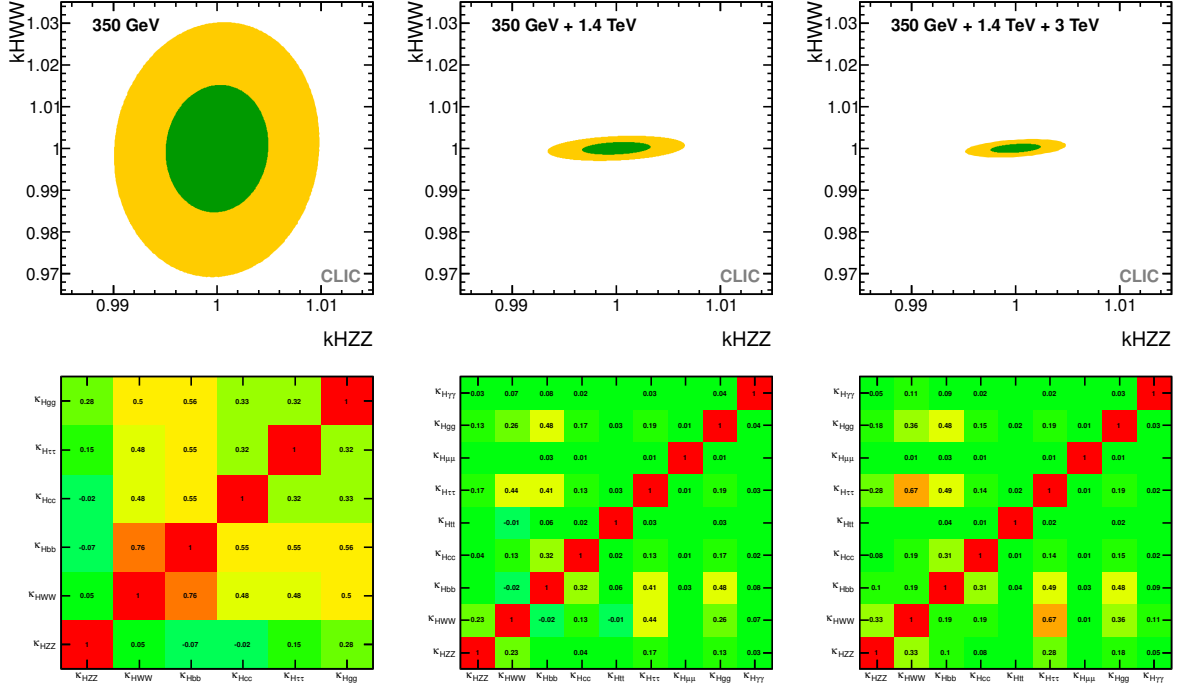


Fig. 2: One and two σ uncertainty contours for κ_{HWW} vs κ_{HZZ} obtained from the model-dependent nine-parameter fit (top) and the full correlation matrix of all fit parameters (bottom).

As in the model-independent case the fit is performed in three stages, taking the statistical errors of CLIC at the three considered energy stages (350 GeV, 1.4 TeV, 3 TeV) successively into account. Each new stage also includes all measurements of the previous stages. Figure 2 illustrates the evolution of κ_{HZZ} and κ_{HWW} and the full correlation matrix of all fit parameters as more measurements at higher energy become available. The total width is not a free parameter of the fit. Instead, its uncertainty, based on the assumption given in Equation 7, is calculated from the fit results, taking the full correlation of all parameters into account. Table 2 summarizes the results of the fit.

To provide an improved comparison to the projected LHC capabilities, the model-dependent fit is repeated with a reduced set of parameters, which uses the assumption of identical coupling deviations of up-type quarks (t, c) and charged leptons (τ, μ), accounting for the difficulties of tagging $H \rightarrow c\bar{c}$ decays at the LHC and the low statistics in the $H \rightarrow \mu^+ \mu^-$ channel. The parameters of this reduced seven parameter fit are κ_{HZZ} , κ_{HWW} , κ_{Hbb} , $\kappa_{H\tau\tau}$, κ_{Htt} , κ_{Hgg} and $\kappa_{H\gamma\gamma}$. Otherwise the fit is performed identically to the model-dependent nine-parameter fit.

Figure 3 shows the full correlation matrix of the fit parameters. Table 3 summarises the fit results.

5. Conclusions

The fit results demonstrate the global precision in the study of the Higgs sector achievable at CLIC in a physics program extending over three energy stages. In a model-independent way, the couplings to vector bosons and to the fermions with branching fractions beyond 1% can be determined with accuracies of 2% to 2.5%, mainly limited by the precision on the coupling to the Z boson. The total width can be

Table 2: Results of the model-dependent fit with nine free parameters. Values marked ”-” can not be measured with sufficient precision at the given energy, while values marked ”< ” have not yet been studied at the given energy, but should result in a considerable improvement of the precision. In the case of g_{Htt} , the 3 TeV case has not yet been studied, but is not expected to result in substantial improvement due to the significantly reduced cross-section at high energy. The uncertainty of the total width is calculated from the fit results following Equation 7, taking the parameter correlations into account.

parameter	precision		
	350 GeV	350 GeV + 1.4 TeV	350 GeV + 1.4 GeV + 3 TeV
κ_{HZZ}	0.49%	0.33%	0.24%
κ_{HWW}	1.5%	0.15%	0.11%
κ_{Hbb}	1.7%	0.33%	0.21%
κ_{Hcc}	3.1%	1.1%	0.75%
$\kappa_{H\tau\tau}$	3.5%	1.4%	<1.4%
$\kappa_{H\mu\mu}$	-	11%	5.2%
κ_{Htt}	-	4.0%	~4.0%
κ_{Hgg}	3.6%	0.79%	0.56%
$\kappa_{H\gamma\gamma}$	-	5.5%	<5.5%
$\Gamma_{H,md,derived}$	1.6%	0.29%	0.22%

Table 3: Results of the model-dependent fit with seven free parameters assuming identical κ s of up-type quarks (t, c) and charged leptons (τ , μ). Values marked ”-” can not be measured with sufficient precision at the given energy, while values marked ”< ” have not yet been fully studied at the given energy, but should result in a considerable improvement of the precision. In the case of g_{Htt} , the 3 TeV case has only been studied for the $c\bar{c}$ final state, but is not expected to result in substantial improvement due to the significantly reduced cross-section of $t\bar{t}H$ production at high energy. The uncertainty of the total width is calculated from the fit results following Equation 7, taking the parameter correlations into account.

parameter	precision		
	350 GeV	350 GeV + 1.4 TeV	350 GeV + 1.4 GeV + 3 TeV
κ_{HZZ}	0.49%	0.33%	0.24%
κ_{HWW}	1.5%	0.15%	0.11%
κ_{Hbb}	1.7%	0.33%	0.21%
$\kappa_{H\tau\tau}$	3.5%	1.4%	<1.3%
κ_{Htt}	3.1%	1.0%	~0.74%
κ_{Hgg}	3.6%	0.79%	0.56%
$\kappa_{H\gamma\gamma}$	-	5.5%	<5.5%
$\Gamma_{H,md,derived}$	1.6%	0.29%	0.22%

determined with a precision of 8.4%. With the assumption that the total width is given by the sum of observable partial widths with variations around SM branching ratios for a Higgs mass of 126 GeV, substantially higher precision is achieved, reaching the per mille to few per mille level for vector bosons and b quarks, and percent to sub-percent accuracy for gluons, τ and charm quarks.

References

- [1] H. Abramowicz et al. Physics at the CLIC e+e- Linear Collider – Input to the Snowmass process 2013. *arXiv:1307.5288 [hep-ex]*, 2013.

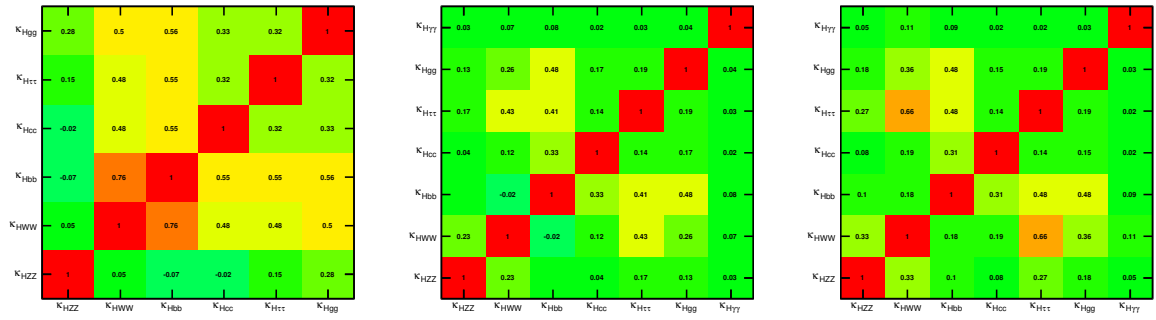


Fig. 3: Full correlation matrix of the seven-parameter model-dependent fit with identical κ s of up-type quarks (t , c) and charged leptons (τ , μ).

Appendices

A. Fit Input

The precision of the σ and $\sigma \times BR$ measurements used in the combined fits are based on full detector simulations with the inclusion of $\gamma\gamma \rightarrow$ hadrons background assuming polarized beam. In time for the Snowmass input documents, not all results were available, so that for some measurements preliminary results or estimates are used. The input data to the fit are summarized in Table A.1. For all measurements above 1 TeV the results from the full simulation studies performed with unpolarized beams have been scaled to account for -80% electron polarization assuming unpolarized positrons. This increases the WW fusion cross-section by a factor of 1.8. It was conservatively assumed that all backgrounds scale by the same factor, which is an overestimate for s -channel processes. The original, unpolarized results are documented in [1]

Table A.1: The precisions obtainable for the Higgs observables at CLIC for integrated luminosities of 500 fb^{-1} at $\sqrt{s} = 350 \text{ GeV}$, 1.5 ab^{-1} at $\sqrt{s} = 1.4 \text{ TeV}$, and 2.0 ab^{-1} at $\sqrt{s} = 3.0 \text{ TeV}$ used in the combined fits. Compared to the unpolarized studies, the results at 1.4 TeV and at 3 TeV have been scaled assuming -80% electron polarization. The majority of the results are from the full detector simulation and reconstruction including overlaid background from $\gamma\gamma \rightarrow$ hadrons. The numbers marked by a * symbol are preliminary and the numbers marked by the † symbol are estimates; these will be updated when full simulation results are available. The – symbol indicates that an a measurement is not possible/relevant at this centre-of-mass energy and “tbd” indicates that no results/estimates are yet available. For the branching ratios, the measurement precision refers to the expected statistical error on the product of the relevant cross section and branching ratio; this is *equivalent* to the expected statistical error of the product of couplings and Γ_H . For the measurement of $t\bar{t}H$, the measurement precisions give the expected statistical uncertainties on the quantities listed under the observable heading.

Channel	Measurement	Observable	Statistical precision		
			350 GeV 500 fb ⁻¹	1.4 TeV 1.5 ab ⁻¹	3.0 TeV 2.0 ab ⁻¹
ZH	$\sigma(\text{HZ}) \times BR(\text{Z} \rightarrow \ell^+ \ell^-)$	g_{HZZ}^2	4.2%	–	–
ZH	$\sigma(\text{HZ}) \times BR(\text{H} \rightarrow \text{b}\bar{\text{b}})$	$g_{\text{HZZ}}^2 g_{\text{Hbb}}^2 / \Gamma_H$	1% [†]	–	–
ZH	$\sigma(\text{HZ}) \times BR(\text{H} \rightarrow \text{c}\bar{\text{c}})$	$g_{\text{HZZ}}^2 g_{\text{Hcc}}^2 / \Gamma_H$	5% [†]	–	–
ZH	$\sigma(\text{HZ}) \times BR(\text{H} \rightarrow \text{gg})$		6% [†]	–	–
ZH	$\sigma(\text{HZ}) \times BR(\text{H} \rightarrow \tau^+ \tau^-)$	$g_{\text{HZZ}}^2 g_{\text{H}\tau\tau}^2 / \Gamma_H$	5.7%	–	–
ZH	$\sigma(\text{HZ}) \times BR(\text{H} \rightarrow \text{WW}^*)$	$g_{\text{HZZ}}^2 g_{\text{HWW}}^2 / \Gamma_H$	2% [†]	–	–
ZH	$\sigma(\text{HZ}) \times BR(\text{H} \rightarrow \text{ZZ}^*)$	$g_{\text{HZZ}}^2 g_{\text{HZZ}}^2 / \Gamma_H$	tbc	–	–
Hv _e $\bar{\nu}_e$	$\sigma(\text{Hv}_e \bar{\nu}_e) \times BR(\text{H} \rightarrow \text{b}\bar{\text{b}})$	$g_{\text{HWW}}^2 g_{\text{Hbb}}^2 / \Gamma_H$	3% [†]	0.23%	0.15%
Hv _e $\bar{\nu}_e$	$\sigma(\text{Hv}_e \bar{\nu}_e) \times BR(\text{H} \rightarrow \text{c}\bar{\text{c}})$	$g_{\text{HWW}}^2 g_{\text{Hcc}}^2 / \Gamma_H$	–	2.2%	2.0%
Hv _e $\bar{\nu}_e$	$\sigma(\text{Hv}_e \bar{\nu}_e) \times BR(\text{H} \rightarrow \text{gg})$		–	1.4%	1.4%
Hv _e $\bar{\nu}_e$	$\sigma(\text{Hv}_e \bar{\nu}_e) \times BR(\text{H} \rightarrow \tau^+ \tau^-)$	$g_{\text{HWW}}^2 g_{\text{H}\tau\tau}^2 / \Gamma_H$	–	2.8%	tbd
Hv _e $\bar{\nu}_e$	$\sigma(\text{Hv}_e \bar{\nu}_e) \times BR(\text{H} \rightarrow \mu^+ \mu^-)$	$g_{\text{HWW}}^2 g_{\text{H}\mu\mu}^2 / \Gamma_H$	–	22%*	12%
Hv _e $\bar{\nu}_e$	$\sigma(\text{Hv}_e \bar{\nu}_e) \times BR(\text{H} \rightarrow \gamma\gamma)$		–	11%*	tbd
Hv _e $\bar{\nu}_e$	$\sigma(\text{Hv}_e \bar{\nu}_e) \times BR(\text{H} \rightarrow \text{Z}\gamma)$		–	tbd	tbd
Hv _e $\bar{\nu}_e$	$\sigma(\text{Hv}_e \bar{\nu}_e) \times BR(\text{H} \rightarrow \text{WW}^*)$	$g_{\text{HWW}}^4 / \Gamma_H$	–	0.8% [†]	0.6% [†]
Hv _e $\bar{\nu}_e$	$\sigma(\text{Hv}_e \bar{\nu}_e) \times BR(\text{H} \rightarrow \text{ZZ}^*)$	$g_{\text{HWW}}^2 g_{\text{HZZ}}^2 / \Gamma_H$	–	2.3% [†]	1.5% [†]
He ⁺ e ⁻	$\sigma(\text{He}^+ \text{e}^-) \times BR(\text{H} \rightarrow \text{b}\bar{\text{b}})$	$g_{\text{HZZ}}^2 g_{\text{Hbb}}^2 / \Gamma_H$	–	1% [†]	0.7% [†]
t \bar{t} H	$\sigma(\text{t}\bar{t}\text{H}) \times BR(\text{H} \rightarrow \text{b}\bar{\text{b}})$	$g_{\text{Htt}}^2 g_{\text{Hbb}}^2 / \Gamma_H$	–	8%	tbd